

Non-edge-ray design: improved optical pumping of lasers

R. John Koschel, MEMBER SPIE
Spectrum Astro, Inc.
3450 East Sunrise Drive, Suite 140
Tucson, Arizona 85718
and
University of Arizona
Optical Sciences Center
Tucson, Arizona 85721
E-mail: john.koschel@osa.org

Ian A. Walmsley
University of Oxford
Department of Physics
Clarendon Laboratory
Parks Road, Oxford, United Kingdom

Abstract. We propose a novel design method for reflective nonimaging concentrators that is based on maximizing system performance beyond standard nonimaging metrics of transfer efficiency and proscribed illumination distribution. This new technique enables system operation characteristics to influence the algorithm, including nongeometrical parameters. This algorithm is termed non-edge-ray design (NERD) because we found that edge rays do not always give optimal illumination design. The case of a diode-pumped, Nd:YAG solid state laser is provided as a confirmation of the design utility. The pump-to-mode configuration, which includes a nonimaging pump cavity reflector, is the focus of this investigation. The merit function of the design process includes not only the transfer efficiency from an extended, 2-D laser diode array, but also the mode coupling of the absorption distribution within a laser rod to its desired output mode. Standard edge-ray design is shown to limit performance, with both numerical and experimental results. Two alternative pump cavity reflectors are developed and the improvements in the outputs from the lasers in TEM₀₀ modes are presented. A periodic cavity sees over 8% improvement in optical efficiency at an output power of 10 W, while an averaging cavity provides nearly 5% improvement. © 2004 Society of Photo-Optical Instrumentation Engineers. [DOI: 10.1117/1.1751400]

Subject terms: nonimaging optics; edge-ray; principle; laser pump cavity; solid-state lasers; illumination.

Paper IE-OE7 received Nov. 11, 2003; revised manuscript received Dec. 10, 2003; accepted for publication Dec. 12, 2003. This paper is a revision of a paper presented at the SPIE conference on Novel Optical Systems Design and Optimization III, Aug. 2000, San Diego, California. The paper presented there appears (unreferred) in SPIE Proceedings Vol. 4092.

1 Introduction

The ability to concentrate light from a source to a target with a desired distribution is often the focus of research or experimentation. Imaging systems, from those with a single lens to more elaborate schemes, such as, for example, Köhler illumination,¹ have been used extensively to accomplish concentration. Typically, the goal of these systems is to illuminate a target object uniformly, while also maintaining a high level of efficiency. Imaging methods worked well for many applications, but they cannot maximize the concentration ratio C , which is defined as²

$$C = \frac{A}{A'}, \quad (1)$$

where A is the surface area of the input beam and A' is the surface area of the output aperture. A stipulation of Eq. (1) is that A' has a shape that it just allows all rays that are transmitted through the optical system between A and A' to emerge from the output aperture. The maximum possible concentration ratio for two-dimensional (2-D) systems and three-dimensional (3-D) systems is

$$C_{2-D} = \frac{n' \sin \theta'}{n \sin \theta} \quad \text{and} \quad (2)$$

$$C_{3-D} = \left(\frac{n' \sin \theta'}{n \sin \theta} \right)^2, \quad (3)$$

where n is the index of refraction in input space, θ is the half-angle in input space, and the primed notation represents output space. The limiting concentration ratio is realized when the output angle θ' is equal to $\pi/2$. With this output angle the concentration ratio is said to be optimal, since all light that enters the optical system at less than or equal to the acceptance angle (i.e., $\theta = \theta_a$) will emerge from the exit aperture (Fresnel reflections, scatter, absorption, or any other such nongeometrical losses are neglected).

Imaging systems suffer from aberrations and limit the output angle value. The aberrations cause light to spill outside the output aperture, thus introducing a geometrical loss. To make the output angle equal to $\pi/2$, the focal length of the imaging system must go to 0. This fact implies that the f -number also goes to zero, which of course means that aberrations completely ruin performance for realistic imaging systems. One lens that can achieve optimal concentration is the Luneberg lens, but it has² an impractical index gradient that ranges between 1 and $\sqrt{2}$. Generally, imaging systems cannot achieve an optimal concentration ratio. If we remove the imaging "constraint," then we can realize maximum concentration. With its removal, we are

no longer constrained to maintain optical path lengths to achieve imaging, but, rather, we require only geometries that efficiently transfer the input light from aperture A to aperture A' . These systems are termed nonimaging.

The field of nonimaging optics removes the imaging condition to achieve a maximum concentration ratio. Light cones or V-trough reflectors are nonimaging designs that, in a sense, started the field.³⁻⁵ This type of concentrator does not achieve optimal concentration, so, alternative algorithms were developed. The first design algorithm to be successful was that of the edge-ray principle and the resulting standard shape of the compound parabolic concentrator² (CPC). The field of nonimaging optics historically developed its start with the introduction^{6,7} of the CPC in 1966. The CPC takes quasi-Lambertian input up to some acceptance angle θ_a and concentrates it into Lambertian output over an output angle of $\pi/2$. This type of concentrator provides a 2-D maximum concentration ratio as can be defined by Eq. (2) and nearly so in three dimensions except for skew-ray losses. The CPC works for planar input and output surfaces, but the edge-ray principle can be extended to account for arbitrarily shaped absorbing surfaces.^{2,8,9} The latter reflectors are called edge-ray concentrators (ERCs). ERCs do not describe the distribution of light if the input is not Lambertian over the acceptance angle. Lambertian emission is not realizable for “real-world” sources so the distribution of light at the target must be determined through propagation methods such as ray tracing. As we see in the next section, this limitation degrades the utility of the edge-ray principle for applications that cannot tolerate caustic formation in the target illumination distribution.

To address this limitation, the nonimaging optics community has investigated a number of novel design methods for tailoring the illumination distribution at the target. These methods maintain use of the edge ray, but enable the acceptance angle to vary across the reflector surface. In these algorithms, the systems have been reversed, such that the source is placed at the previously described “output aperture” and the illumination distribution is determined at an arbitrary target plane. Rather than being called concentrators, they are called illuminators. This work—usually termed tailored edge-ray design (TED)—has been developed extensively over the past decade, with the following developments: tailored illumination in the far field,^{10,11} near-field tailored illumination taking into account the angular source emission distribution,¹² and free-form optical surfaces for arbitrary illumination distribution forms.¹³ These techniques have been useful for expanding the field of nonimaging optics, but they all describe the calculation of the irradiance distribution at a target plane or intensity distribution if the far field is required. It is not overly complex to extend the methods to nonplanar target surfaces; however, none of the methods can easily be extended to account for absorption over a volume rather than on a surface. Rather than trying to obtain a surface distribution of light (i.e., irradiance), the goal would be the volumetric absorption distribution (i.e., power density). There are a number of applications where power density is required, such as optical pumping of a solid state gain medium that is the focus of our investigation. In our investigation, we use the concentrator design algorithm, such that we surround

the target volume with a reflector. With standard nonimaging design methods using the edge-ray principle, one can calculate and design for some prescribed distributions across the surface of the target, but further ray tracing is required to determine the volumetric absorption distribution. In fact, as is shown in the next section, a standard ERC forms caustics within the absorbing volume of a cylindrical absorber. Edge-ray design methods are too constrained to provide a desired absorption distribution over a volume. Methods that enable variation of the acceptance angle as a function of position on the reflector in conjunction with a target position within the volume give the most control to provide a volumetric absorption distribution.

We propose a new algorithm that takes into consideration the desired volumetric absorption distribution at the target. There are numerous applications of when the absorption distribution within the volume is beneficial, and we will use the example of a high-output-power, diode-pumped, solid-state laser rod to highlight the design technique. We will develop a pump configuration that maximizes performance of the laser in the TEM₀₀ mode. There are essentially two pump configurations, end pumping and side pumping, which can then be further delineated to account for the details of each pumping scheme. End pumping refers to the case when the pump radiation is collinear with the resonator axis, while side pumping describes the situation when the pump radiation is directed at an angle to this axis, typically, on average, orthogonal to it. End pumping is typically used when high efficiency is the primary goal, whereas side pumping is better suited to high-power operation. The side-pumped geometry enables a large amount of pump power to be transferred to the surface of the gain medium.^{14,15} The reason for the increased efficiency of end pumping is that pump power is absorbed over a small, centered region within the laser rod leading to a much higher inversion density than in side pumping, where a sizable amount of the pump power is absorbed near the surface, not the center, of the gain medium. The highest inversion density in a region the same size or smaller than the fundamental mode is the deciding factor for low threshold and high optical efficiency^{16,17} (hereafter we call the limit of equal-sized gain and mode distributions mode matching). Because we are looking for a high-output-power configuration, side pumping is preferred. Close-coupled, side pumping of a laser rod is the best configuration for obtaining mode matching in a side-pumped geometry, but this configuration is limited by the number of diode pump sources that can be located in proximity to the laser rod.¹⁵ Thus, we investigate high-power pump configurations for which the diode lasers can be situated in a single extended planar array and then their emission transferred to the laser rod via a single reflector and no other intervening optics. This requirement points naturally to nonimaging concentrators that have been introduced already. Pump configurations employing nonimaging cavities have been proposed or developed previously, but most of these investigations has investigated the coupling of the gain distribution to the laser performance.^{15,18,19} Only recently has the subject been considered for the optimization of laser performance.²⁰

In the next section, we discuss the modeling method in more detail. We also investigate the use of an ERC to accomplish our goal of high output power from the laser

when using an extended laser diode array. Finally in this section, we provide experimental results of the multimode laser performance and compare the fluorescence measurements to that of our models. In the third section, we develop the theory for improving performance of a high-power Nd:YAG laser using reflectors that account for volumetric absorption requirements. In the fourth section, we report performance for two new designs that use the non-edge-ray design (NERD) method. The first is a periodic pump cavity (PPC) for coupling the extended, 2-D laser diode array into the laser rod volume. The second is an averaging pump cavity (APC). It is shown that the PPC provides better laser performance than the APC and ERC, but at the expense of a more complex pump cavity shape. Finally, in Sec. 5 we list conclusions, discuss fabrication issues, and indicate future research that can be conducted in this field.

2 Discussion and Validation of Modeling Method

Unless noted otherwise in the text here, the following techniques and parameters are used to model the laser. Using ray tracing and incremental absorption along the path of each ray we can determine the absorption distribution within a solid state gain material.¹⁵ The examples within this paper use a 6.35-mm-diam Nd:YAG laser rod as the gain medium. The outer surfaces of the laser rod are modeled as uncoated, smooth, and specular. We use a 1.1% doped Nd:YAG rod for our examples, which provides a modeled absorption coefficient of 0.4 mm^{-1} at the peak diode-pump line of 808 nm. It is assumed that the diode array is cooled such that each diode emits at 808 nm. One can modify the model by adding a weight term for each emitter in the array if it is not emitting at 808 nm. All reflectors in this study are smooth, specular, and coated with gold, which has a 99% reflectivity at 808 nm. After the pump light is absorbed within the gain medium, the coupling to the laser mode is calculated.¹⁷ This step involves prescribing the mode distribution while using the absorption distribution determined within the ray-tracing step. Note that the gain distribution is equal to the absorption distribution multiplied by the upper state efficiency of the gain material, which is 72.2% for Nd:YAG. Finally, an optimizer is added to the mode coupler analysis to determine the optimal TEM₀₀ mode for the determined gain distribution.¹⁷ We discuss the model in more detail in the next two subsections. In Sec. 2.3 we provide a numerical example of the model using an ERC for a circular absorber. Section 2.4 provides validation of the ray-trace model, while Sec. 2.5 discusses the limitations of the ERC for diode-pumping schemes.

2.1 Absorption Distribution Calculation

The absorption distribution is calculated with the protocol provided in Ref. 15. First the source is modeled. Each diode emitter in the full 2-D array has an elliptical Gaussian emission with FWHM divergence angles of 10 deg in the direction of the bars and 40 deg perpendicular to the bars. Each emitter is modeled as a point source for the purpose of this study. No phase information is retained for the diode radiation, thus an incoherent ray-trace model can be used. A deterministic set of rays is traced in three dimensions from each of the emitters. Dividing the angular emission profile

into a set of bins determines the selection of the rays. The area under the angular emission profile for each bin is equal, thus this method traces more rays in the directions of the peak emission. Each ray is given a power of $P_{\text{diode}}/N_{\text{rays}}$, where P_{diode} is the actual emitted power of each emitter, and N_{rays} is the prescribed number of rays that is traced from each diode—around 65,000 rays are traced for each emitter.

The diode array is oriented such that the 10-deg direction is along the axis of the laser rod and the 40-deg direction is perpendicular to it. Next the rays are traced according to the law of reflection at the pump cavity surface and Snell's law at the interface of the laser rod. The side of the rod has an uncoated, polished surface that introduces Fresnel losses. Only the transmitted rays are traced, thus no Fresnel reflections are included in this model. The gain medium is sectioned into a number of polar bins (i.e., comprised of radial rings and angular spokes). The laser rod is not binned along its length in the low-gain limit since the integration of gain along the length of the rod can be used. As the rays propagate through each of the bins in the laser rod, the absorption is calculated within each bin dependent on the path length within the bin and absorption coefficient. All rays will exit the gain medium, but they are stopped once only 5% of their original flux remains. Rays that do not meet this stopping condition continue their propagation within the pump cavity. This step enables rays to reenter the gain medium, but usually most exiting rays will be ejected from the pump cavity. Ejection occurs when the rays are incident on the plane of the diode array. The summation of the absorbed power for all rays within each bin determines the absorption distribution.

2.2 Mode-Coupling Calculation

Once we find the absorption distribution, it is multiplied by the upper-state efficiency to determine the gain distribution. Next, using the low-gain limit, which limits a quasi-cw laser to an output coupler of 30% maximum transmissivity, one can calculate the optical efficiency of the laser for a prescribed transverse mode.¹⁷ The equation governing the mode coupling is

$$\frac{1}{P_{\text{in}}} = \frac{4\eta_U}{P_{\text{sat},r}L} \int_0^{2\pi} \int_0^\infty \frac{g(r,\theta)f(r,\theta)/A_p}{1+4P_{\text{out}}f(r,\theta)/P_{\text{sat},r}T_{\text{oc}}} r \, dr \, d\theta, \quad (4)$$

where P_{in} is the absorbed optical input power, P_{out} is the optical output power, $P_{\text{sat},r}$ is the saturation power related to the mode area, A_p is the pump area, $g(r,\theta)$ is the absorption distribution, $f(r,\theta)$ is the mode distribution, η_U is the upper-state efficiency, and L is the roundtrip loss factor. Typically, the mode distribution is that of a TEM₀₀ mode (i.e., Gaussian), but one can investigate single higher order mode behavior or multimode output¹⁷ (i.e., when the mode distribution equals that of the gain distribution). Equation (4) provides the metric for optimization of laser performance: for a provided input power, the output power is to be maximized. Another expression of this is the optical efficiency

$$\eta_{\text{opt}} = \eta_c \eta_U \eta_m = \frac{P_{\text{out}}}{P_{\text{in}}}, \quad (5)$$

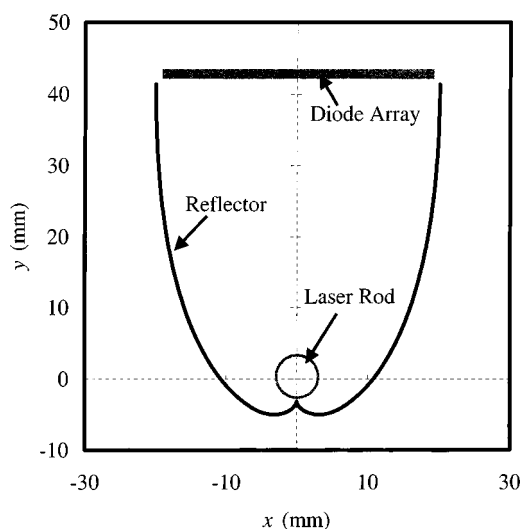


Fig. 1 Cross section of the ERC for a circular absorber featured in Sec. 2.5. Also shown are the laser rod and the bars of a 2-D laser diode array. The ERC pump cavity is made by extruding this cross section along the length of the laser rod.

where η_{opt} is the optical efficiency, η_c is the pump-coupling efficiency (as determined with the algorithm of Sec. 2.1), and η_m is the mode-coupling efficiency [as determined through Eq. (4)]. An optimizer can be included in the mode-coupling calculation to optimize the mode selection for the modeled absorption distribution.¹⁷ In this case, one typically minimizes the inverse of Eq. (5) (i.e., $1/\eta_{\text{opt}}$). Typical variables for this type of optimization include the fundamental mode radius, the transmission of the output coupler, and the axis location of the resonating mode with respect to the axis of the laser rod. Diffraction of the resonating mode is included in the model, such that typical optimal mode configurations locate the mode axes along the laser rod axis. Additional parameters can be included in the modeling, including parameters that denote the pump configuration, such as the diode spacing, radius of the laser rod, and acceptance angle of the nonimaging pump cavity.²¹

2.3 ERC Example

Figure 1 depicts the cross-sectional shape of an ERC for a circular absorber. Extruding this cross section along the length of the laser rod forms the ERC pump cavity. The one displayed in Fig. 1 is the functional shape for the ERC discussed in Sec. 2.5. This reflector is designed with two variables: the radius of the laser rod and the acceptance angle of the concentrator. All parameters are as denoted previously, except the angular emission characteristics of the diode arrays. Up to two McDonnell Douglas (MDAC) 25-bar arrays with FWHM 40×10 -deg angular emission patterns are used. The term “bar” denotes a single linear array of laser diodes. The term “25-bar” denotes that 25 of these linear arrays are stacked upon each other to create a 2-D array of laser diode emitters. The 25-bar MDAC arrays have a diode spacing of 0.28 mm between bar centers and 0.143 between cluster centers along each bar. The surface area of each array was 1 cm^2 . The arrays are operated at 2 Hz with $200\text{-}\mu\text{s}$ pulses. The ERC reflector and laser rod

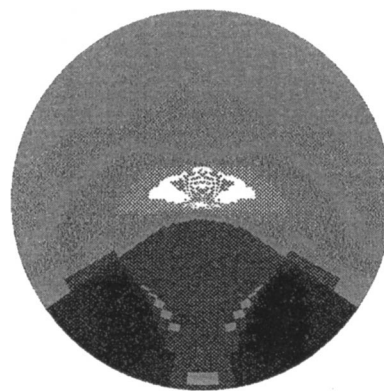


Fig. 2 Modeled absorption distribution for a single 25-bar MDAC diode array positioned 42 mm above the optical axis of the Nd:YAG laser rod.

lengths are 15 mm. Flat, gold-coated plates enclose the ends of the pump cavity. Optimization of the variables for the resonator and pump configurations give the following results:

1. diode array position: centered at a distance of 42 mm above the optical axis of the rod
2. ERC acceptance half-angle: 30 deg
3. mode axis: along the optical axis of the laser rod
4. high-reflection reflector: 5-m radius of curvature
5. output coupler: 97% reflection and 3% transmission, 51-cm radius of curvature
6. resonator cavity: 7 to 10 cm in length.

Modeling results for a single 25-bar MDAC array being used as the pump source showed that about 75% of the pump light would be absorbed within the laser rod, the upper-state efficiency is 72.2% for Nd:YAG, and the mode-coupling efficiency is 22% for multimode operation and 10% for TEM_{00} operation. These parameters and Eq. (5) give modeled optical efficiencies of 11.9% for multimode operation and 5.4% for TEM_{00} operation at an output energy of 20 mJ. The modeled absorption distribution for pumping with a single 25-bar MDAC array is shown in Fig. 2. Figure 3 shows the experimental output energy as a function of input energy [i.e., energy out of the diode laser array(s)] when one and two 25-bar MDAC arrays are used to pump. When two 25-bar MDAC arrays are used there is a gap of 8 mm between the two arrays. This gap is positioned directly above the laser rod at a distance of about 42 mm from the optical axis of the laser rod. The multimode output for the single array pump case is superimposed on Fig. 3. For the case of a single 25-bar MDAC array, the measured optical efficiency of the multimode output was 10% at an output energy of 19.9 mJ, and analogously 5% into the fundamental mode of the resonator. The TEM_{00} operation has excellent agreement between the model and experiment. The multimode behavior is 20% lower for the experiment in comparison to the model, which is likely due to a near-hemispherical resonator being used. The multimode model assumes a dual-planar resonator, but this configuration was not set up in the laboratory.

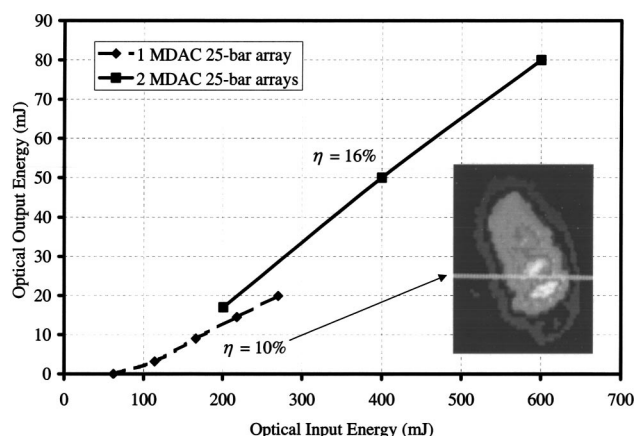


Fig. 3 Experimental measurement of the optical output energy versus optical input energy for one and two 25-bar MDAC laser diode arrays. Superimposed is the multimode output for the cavity described in Sec. 2.3.

Finally, the ERC design has an aperture of about 42-mm across. Thus, in theory over four of these 25-bar MDAC arrays can be located in the aperture. Underfilling of the aperture leads to the formation of caustics in the laser rod, which is evidenced by the modeled absorption distribution of Fig. 2. The formation of these caustics remains even for an array that spans the entire input aperture, but to a lesser extent. This phenomenon is due to the nature of the angular emission of the diode lasers. To reduce the caustics, the emission of the source radiation would have to be both uniform in position and angle. This topic is discussed further in Sec. 2.5.

2.4 Validation of the Absorption Model

The experimental results of the previous section help to validate the model that has been developed; however, we felt it prudent to verify the ray-tracing algorithm that has been developed. To do this we used a 4-bar MDAC array with the same emission characteristics as listed in Sec. 2.3, but in this experimental study no resonator was placed around the gain medium. We then imaged the fluorescence from the Nd:YAG laser rod onto a CCD and compared the results to models of the absorption distribution at three lateral locations of the 4-bar array (see Fig. 4): 0.0 mm (i.e., directly above the laser rod at a distance of 42 from the laser rod axis), 10.0 mm, and 19.0 mm. Figure 4 shows good agreement between the model [i.e., Figs. 4(a), 4(c), and 4(e)] in comparison to their respective experimental measurements [i.e., Figs. 4(b), 4(d), and 4(f)]. Discrepancies between the model and experiment are most likely due to uncertainty of the exact lateral position of the 4-bar array in the experimental case. This experiment also indicated that the selected source model technique is appropriate for individual emitters in a laser diode array, especially that the emitters can be treated incoherently. Finally, Fig. 4 provides a better understanding of how the caustics form due to position of the diodes and their angular emission profile.

2.5 Limitations of the ERC Pump Cavity

As noted in Secs. 2.3 and 2.4, caustics form within the laser rod due to the underfilling of the input aperture both in

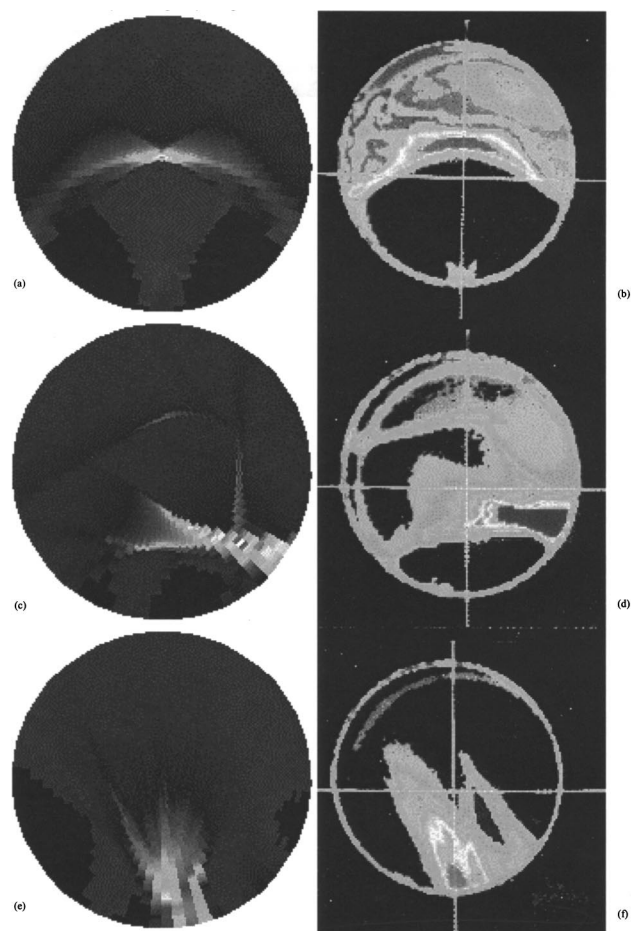


Fig. 4 Absorption distribution model and the measured fluorescence from a 6.35-mm diameter Nd:YAG laser rod with a 4-bar MDAC array at three transverse locations in the input aperture. Modeling: (a), (c), and (e) at 0.0, 10, and 19 mm, respectively; and experimental: (b), (d), and (f) at 0.0, 10, and 19 mm respectively.

angle and position. Simply said the base shape of the ERC for a circular absorber is not optimal for diode-pumping applications. Figure 5 shows the absorption distribution for the ERC shown in Fig. 1. The diodes span the entrance aperture with a spacing of 1.0 mm, which results in 41 individual diodes in the cross section of the pump cavity. Figure 5 shows that the maximum gain region is located in the lower portion of the laser rod, near the cusp of the concentrator. Ray tracing indicates that 75% of the pump light is absorbed within the gain medium. This location is not optimal for operation of the laser in the TEM₀₀ mode, for two reasons. First, diffraction of the laser mode from the edges of the gain medium reduces the effective gain. Second, the ERC leads to localized Lambertian illumination on the surface of the laser rod due to the underfilling of the input aperture. This in turn leads to localized ray concentrations within the gain medium. Such hot spots are problematic, giving rise to thermal birefringence, increased amplified spontaneous emission (ASE), fracture, and coupling to undesired spatial modes. It would therefore be useful to seek a concentrator design that enables more precise control of the pump absorption distribution in the gain medium, in particular one that enables preferential pumping of the desired spatial mode and a corresponding reduction of

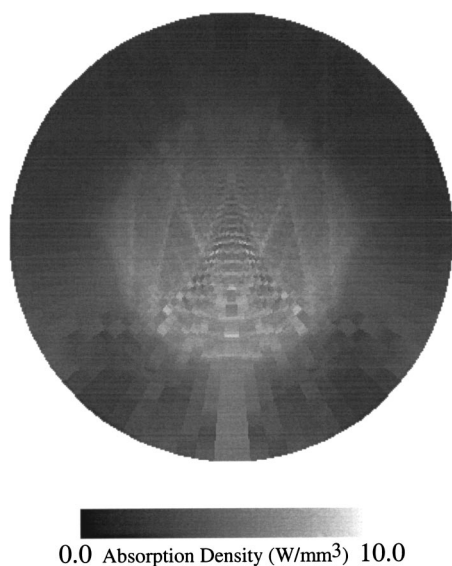


Fig. 5 Absorption distribution for a Nd:YAG laser rod within the ERC shown in Fig. 1. The laser rod is pumped with a diode array with the parameters listed in Secs. 2 and 2.1. The diodes span the entrance aperture of the ERC and have a spacing of 1.0 mm.

the gain in undesirable modes. The literature is in agreement with these points: “The beam overlap efficiency η_B describes the spatial overlap between the resonator modes and the pump power, or gain distribution of the laser medium. In an amplifier, η_B is a measure of the spatial overlap of the input beam with the pump or gain distribution in the laser material. This subject usually does not receive a lot of attention in the laser literature, but a poor overlap of the gain region of the laser with the laser-beam profile is often the main reason why a particular laser performs below expectations.”²²

The limitation of all ERCs is that only a few parameters are used to make the design: radius of the absorber and acceptance angle. This limited set of parameters cannot provide optimal mode overlap with the gain profile, or in other words, the volumetric absorption distribution within the gain medium cannot be optimized. Additional parameters such as the location of discrete emitters and their angular emission profiles are not taken into account. TEDs provide a little more control, but they also do not describe the propagation through an absorbing target. The end result is that TEDs do not solve the problem either, so there is no reason to investigate them further. A novel design algorithm must be proposed and developed for volume targets. The next section provides the base theory for such circumstances.

3 NERD Theory

The major premise of the ERC from the previous section is that all rays up to a certain fixed acceptance angle are transferred to the output surface (in our case the outer surface of the laser rod). Rays entering the concentrator aperture at greater angles are turned back after several reflections. For instance, the concentrator for the absorption distribution in Fig. 2 had an acceptance angle that passed 95% of the diode radiation to the laser rod surface. While this principle works well for sources of low divergence radiation (such as

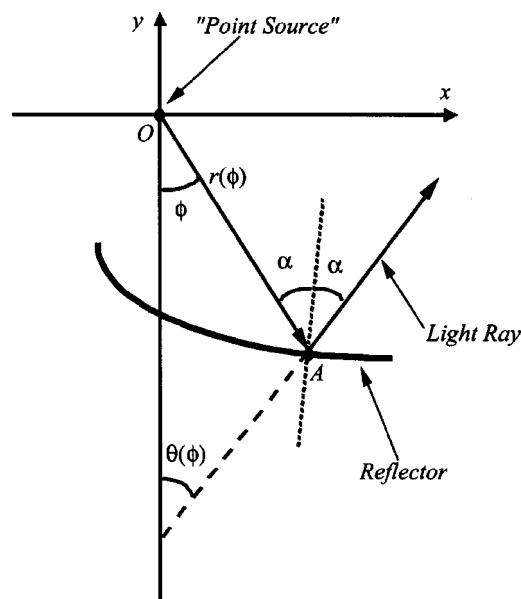


Fig. 6 Geometry for finding the reflective surface of a NERD pump cavity. Note that the system is designed in reverse by placing a virtual “point source” at O and propagating the “emitted” light to the far field. In actuality the optical axis of the laser rod is located at O and source is placed above the laser rod. This inverse method eases the design process.

the sun), it is not optimal for sources with even moderately divergent beams, since the design anticipates that rays striking the concentrator surface at any point have similar azimuthal angles. What is required is a design in which the acceptance angle is a function of the position on the reflector and a target point at the absorber, such that the étendue is still maximized, but simultaneously each section of the extended pump source is partially imaged at the selected target point within the laser rod. There is, of course, ultimately a trade-off between high concentration, good imaging, and input aperture size, and it is that compromise we explore here.

Our starting point is an algorithm that constructs a TED reflective surface that produces a desired far-field irradiance distribution from a line source.¹⁰ This method makes use of the geometry shown in Fig. 6, where O locates the position of a “point source” in the x - y plane at the origin, α is the angle of incidence of the ray on the reflector and is therefore also the reflection angle, $r(\phi)$ is the distance from the origin to the reflector surface as a function of the polar angle ϕ measured from the negative y axis, and $\theta(\phi)$ is the output angle after reflection at point A . The angular output distribution $\theta(\phi)$ also denotes the intensity distribution. Figure 6 is the reverse of what is actually used in our system; the “point source” at O is located on the axis of the resonator while $\theta(\phi)$ is the angular input distribution from the extended diode array. The equation that governs the surface is the law of reflection in polar coordinates,

$$\frac{d \ln[r(\phi)]}{d\phi} = \tan(\alpha) + \frac{a}{r(\phi)}, \quad (6)$$

where, for complete generality, a is the radius of a “source” centered at O (or, in our setup, the radius of the

laser rod). As per Refs. 16 and 17, the optimal pumping scheme occurs when the absorption distribution width is minimized. To achieve this scheme, we need to image as much pump radiation to the center of the laser rod (i.e., pseudo-imaging). Setting the radius of the “source” to 0, and integrating Eq. (6) provides the shape of the reflector,

$$r(\phi) = r_1 \exp \left\{ \int_{\phi_1}^{\phi} \tan \left[\frac{s - \theta(s)}{2} \right] ds \right\}, \quad (7)$$

where r_1 is the distance along a prescribed angular direction ϕ_1 , and s is the variable of integration denoting the angular position on the reflector surface. Typically, ϕ_1 is chosen to be along the negative y axis. Equation (7) enables the acceptance angle $\theta(s)$ to be tailored over the extent of the reflector. From the tailored edge-ray design (TED), by making the edge ray adaptive over the extent of the reflector one can tailor the far-field irradiance distribution to compensate for such physical phenomenon as the cosine falloff across a target plane illuminated by a source.¹¹ Because we use the edge ray, a sharp cutoff in the intensity distribution is maintained while being able to address the distribution of light to a small degree.

It is not necessary to restrict the interpretation of Eq. (7) such that $\theta(s)$ is prescribed by the edge-ray angle, but rather it can be an interior ray (i.e., non-edge-ray) dictated by the geometry and desired performance of the illumination system (e.g., laser performance). By using an interior ray the sharp cutoff in the intensity distribution at the target plane is lost, but we gain the benefit of further control of the light upon reflection. Because we no longer hold the edge-ray as the important ray for the design process but some interior ray, the design algorithm is termed NERD. In the next section, two concentrator examples in the field of diode-pumped, solid state lasers are shown. In each case, the choice of $\theta(s)$ is chosen to minimize the width of the volumetric absorption distribution in conjunction with the geometry of the system and characteristics of the source and target. The distribution $\theta(s)$ is also called the aim function.

4 NERD Examples

The choice of the aim function must address optimizing the merit function for the application. For the case of a diode-pumped, solid state laser rod, it was shown in Refs. 16 and 17 that as the width of the pump distribution is decreased in comparison to the mode distribution, better laser performance is obtained. Thus imaging methods to direct the radiation from each laser diode to the center of the laser rod are desired. This optical system is unobtainable with an extended, 2-D diode array due to conservation of étendue. Two lesser, but possible, solutions are possible:

1. Each point on the reflector surface preferentially addresses a single laser diode, or
2. Each point on the reflector surface looks at the diode array as whole and determines the location of a composite source point in the array.

The first choice provides a PPC and is described in the next

section. The second option is an APC and is described in Sec. 4.2. Section 4.3 compares the modeled performances of the ERC, the PPC, and the APC.

4.1 PPC

An appealing solution is found by using a single reflective surface for which the surface is divided into segments, with each segment being used to control preferentially the output of an individual emitter. The rays associated with direction of the largest power propagation (i.e., the rays emitted orthogonal to the diode laser surface) are then directed to the center of the laser rod. Neighboring rays are directed close to the center of the laser rod, thereby increasing the absorption density at the laser rod center. Since there are several discrete emitters to be imaged to O , we consider a PPC profile such that the reflection angle at its surface given by

$$\theta(\phi) = \theta_0 f[\sin(A\phi)], \quad (8)$$

where θ_0 is the maximum reflection angle, $f[\sin(A\phi)]$ is a function of the polar coordinate angle, and A is an arbitrary factor such that there are A periodic segments in π rad. The emitters are placed in the aperture of the reflector at the x positions such that $\theta(\phi) = 0.0$. A reflector surface with the functional form of Eq. (8) is rippled, or rather, it is said to be stimped. As a potential solution we use

$$\theta(\phi) = \theta_0 \sin^2(A\phi). \quad (9)$$

Substitution of Eq. (9) into Eq. (7) is not solvable analytically, so the solution is found numerically through an iterative approach. The iterative approach uses a guess for a point on the reflector. A series of corrections are made to this guess till the change between successive iterations is sufficiently small. This point is then stored for future look up during ray tracing while also providing the guess for the next point on the reflector. On ray tracing to find the absorption distribution within the gain medium, neighboring stored points bracket any intercept on the reflector surface. This method greatly speeds up the process of finding the final reflective surface, especially during complex ray traces. Note that Eq. (9) is positive valued or zero over the range of ϕ . This choice ensures that the reflected rays are not alternating from one side of the optical axis to the other over each oscillation. Such oscillations have been noted to cause detrimental overall performance of the illumination system. While the sparse nature of the discrete diode emitters maintains an underfilled entrance aperture, we have now localized “imaging” distributions of light on the surface of the laser rod. In other words, the illumination distribution from each diode has its centroid directed toward the center of the laser rod. This result will reduce the caustic formation within the laser rod while providing a smoother absorption distribution that increases toward the center of the laser rod.

Shown in Fig. 7 is a cross section of the PPC obtained when $A = 20$, $\theta_0 = \pi/6$, $\phi_1 = 5\pi/6$, and the diameter of the Nd:YAG laser rod is 6.35 mm. The axes denote the dimensions of the PPC curve shown in the foreground. Note that the spacing between the locations where $\theta(\phi) = 0.0$ is not constant so that the diodes do not have a uniform spacing. The nonuniform spacing simply requires that the submount

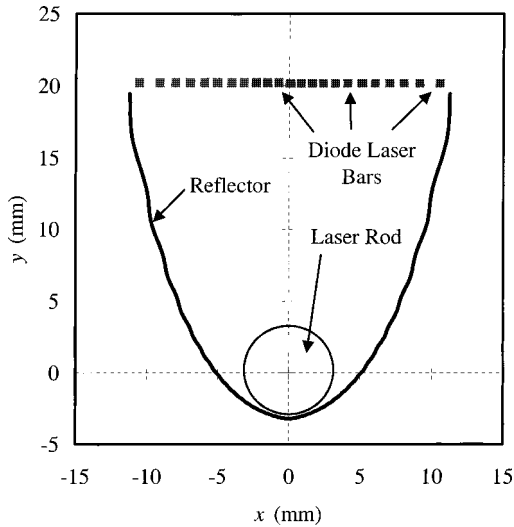


Fig. 7 Cross-sectional profile of the PPC developed in Sec. 4.1. The PPC pump cavity is made by extruding this cross section along the length of the laser rod.

thickness between consecutive bars must be unequal, so that the diodes are spaced more widely near the edges of the input aperture. For $A=20$ there are 33 diodes in the entrance aperture of this PPC. Extruding the cross section shown in Fig. 7 along the length of the laser rod provides the pump cavity. Figure 8 shows the pump absorption density distribution for the PPC. The diode array pump sources used in the design are pulsed, 1-cm linear bars that emit a peak power of 50 W. Individual diodes radiate into a FWHM 40×10 -deg angular distribution with the broad angle arranged orthogonal to the gain medium axis. Notice that the pump distribution is more uniform for the PPC in comparison to that shown for the ERC in Fig. 5 (note that the same scales are used in Figs. 5 and 8). Additionally, with fewer caustics, their deleterious effects on laser per-

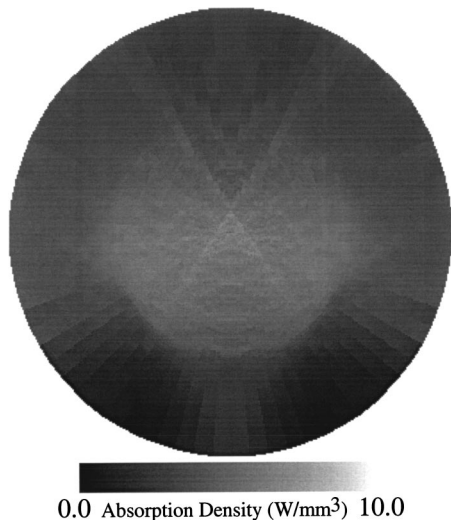


Fig. 8 Modeled absorption distribution for the PPC shown in Fig. 7. The laser diodes are positioned in the entrance aperture of the PPC above the centers of each one of the ripples.

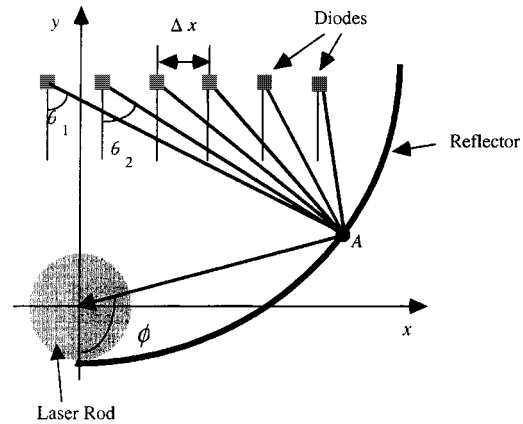


Fig. 9 Geometry for determining the weighted average angles for the APC.

formance are greatly reduced. Finally, ray tracing indicates that 72% of the pump light is absorbed within the gain medium.

4.2 APC

While the shape of the PPC can be manufactured with techniques such as electroforming or injection molding, its tolerance requirements will prove demanding. The design conditions of the PPC dictate the rippled profile. A more manufacturable shape is one that while considering the emission properties of the diode array does not have a periodic structure. This design condition is accomplished by summing up the ray angles from each laser diode to the virtual intercept on the reflector surface (see Fig. 9). The reflector surface point is virtual because an iterative approach must be used to determine the actual intercept: first a guess is made with the use of the previous reflector point and this guess is refined through iterations till the tolerance is sufficiently small. The power directed along the ray path from each of the diodes to the virtual reflector surface point is used to weight the diode ray angle. The weight terms are normalized such that a weight value of 1.0 is obtained for a ray path along the peak emission direction (i.e., along the y axis due to the source model and selected geometry). This construct can be expressed in functional form by

$$\bar{\theta}_A = \frac{\sum_{n=0}^N w_n \arctan[(x_A - x_d + n\Delta x)/(y_A - y_d)]}{\sum_{n=0}^N w_n}, \quad (10)$$

where the weighting factor is given by $w_i = P_d(\theta_i)/P_d(\theta = 0)$, $N + 1$ is the number of diodes, (x_d, y_d) is the location of the central diode, (x_A, y_A) is the intercept location on the reflector surface, Δx is the constant diode spacing, and $P_d(\theta)$ is the power of the laser diode along the ray angle θ . The choice of averaging the ray angles from the many laser diodes gives this reflector its name: APC. Using Eq. (10) in conjunction with Eq. (7) the cross-sectional shape as shown in Fig. 10 is determined. Note that there are no periodic structures, which alleviates fabrication concerns. Once again extruding this cross section makes a trough.

Using the parameters listed in the previous sections the modeled absorption distribution in a Nd:YAG laser rod for

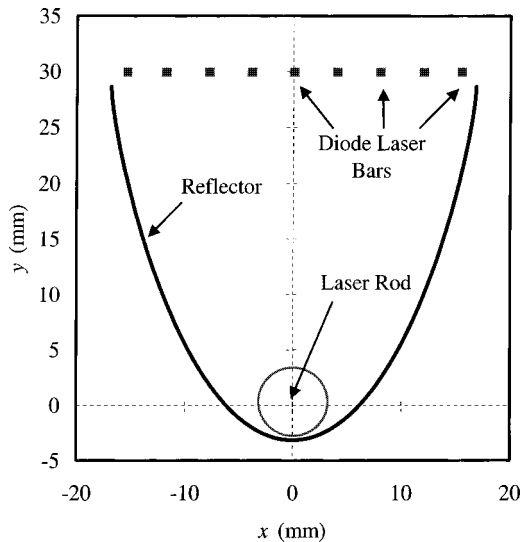


Fig. 10 Cross-sectional profile of the APC developed in Sec. 4.2. The APC pump cavity is made by extruding this cross section along the length of the laser rod.

the APC is shown in Fig. 11 (note that the same scales are used in Figs. 5, 8, and 11). Once again caustic formation is greatly reduced, in fact analysis shows that the APC provides the smoothest absorption distribution. The APC gives a slightly worse transfer efficiency, 70%, as compared to the other pump cavities, but as will be seen the coupling to a TEM_{00} mode is better.

4.3 Comparison of Pump Cavity Geometries

To gauge the effectiveness of the pump cavities designed with NERD, the method of Sec. 2.2 is employed to calculate and optimize the optical efficiency with TEM_{00} output of a laser at a given output power and absorption distribution: ERC (Fig. 5), PPC (Fig. 8), and APC (Fig. 11). Figure 12 shows the output power versus the input power for these three pump cavities. Table 1 provides the input power, optical efficiency, and improvement over the ERC design for

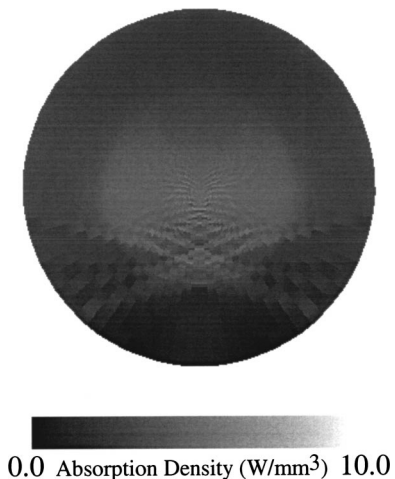


Fig. 11 Modeled absorption distribution for the APC shown in Fig. 10. The laser diodes are positioned in the entrance aperture of the APC with a spacing of 1.0 mm.

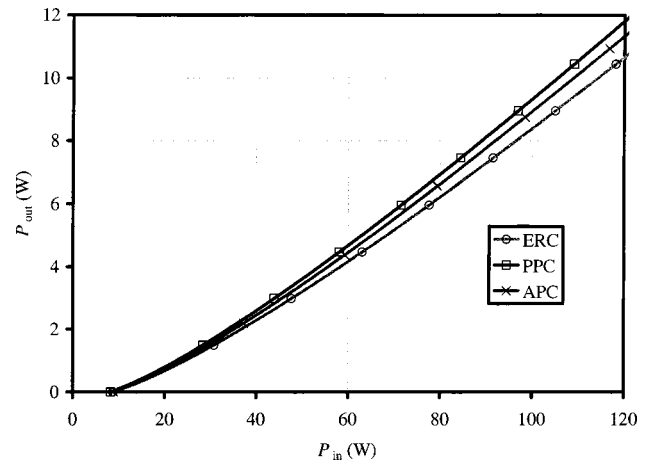


Fig. 12 Output power versus input power for the three absorption distributions: ERC (Fig. 5), PPC (Fig. 8), and APC (Fig. 11). Note that the laser rod characteristics and angular emission pattern of the diodes are the same for all three pump cavities.

two target output powers (1.0 and 10.0 W) for the ERC, PPC, and PPC pump cavities. Note that the input power is the optical pump power required to obtain the designated output power. The optical efficiency at a target output power of 10 W is 9.48% for the PPC and 9.18% for the APC compared to 8.75% for the ERC, which means the PPC has improved on the ERC by 8.29% and the APC has improved by 4.87%. These increases in the optical efficiency are due to the higher absorbed pump power density at the laser rod center, as shown in Fig. 13. The radially summed absorption distribution for the ERC, PPC, and APC cavities are shown in this figure in addition to an analytic model that assumes Lambertian illumination of the laser rod surface.²³ This figure shows the sum of the absorbed pump power density within a sequence of radial rings of equal area. Notice that the ERC follows the analytic model rather well, while the PPC and APC deviate from it—there is a higher pump density at the center of the laser rod ($r/a=0.0$). This indicates that the PPC and APC direct a significant amount of the pump radiation toward the center of the laser rod, yielding a gain distribution that more closely matches the optimum for the fundamental mode of the cavity. Due to considering each diode emitter separately the PPC directs more power toward the center of the laser rod in comparison to the APC.

5 Conclusions and Future Research

The NERD technique provides a robust method to design reflectors in the near field by taking into account application, source, reflector, and target characteristics. Edge-ray design takes into account two aspects of the system, constant acceptance angle and shape of the absorber. TED introduces other considerations such as aiming of the edge ray and variation of the edge-ray angle across the reflector surface; however, it is fundamentally limited to use of the edge ray. We have shown a case where using nonedge rays improve on the system performance. The motivating factor is that the volume absorption distribution is important rather than the surface absorption distribution. Due to the use of discrete laser diode emitters as the pump source, the

Table 1 Input power, optical efficiency, and improvement over ERC design at two target output powers (1.0 and 10.0 W) for ERC, PPC, and APC.

	$P_{\text{out}} = 1 \text{ W}$			$P_{\text{out}} = 10 \text{ W}$		
	P_{in} (W)	η (%)	Improvement (%)	P_{in} (W)	η (%)	Improvement (%)
ERC	24.52	4.08	0.00	114.22	8.75	0.00
PPC	22.59	4.43	8.54	105.48	9.48	8.29
APC	23.56	4.24	4.08	108.92	9.18	4.87

aperture will be underfilled, which, when using standard edge-ray designs, leads to a poor volume absorption for mode coupling due to caustic formations away from the center of the laser rod. A better approach is to redirect the pump radiation to desired locations within the absorption volume. Though we used a basic example, pseudo-imaging of an array of diode emitters to the center of the laser rod, it highlights the differences between TED and NERD. Using the PPC example, TED would have imaged within each segment of the reflector, the edge ray from each of the diodes to the center of the laser rod. In NERD, it images the most powerful ray (the central one in this case) to the laser rod axis, while the edge ray is transferred to some position around the central ray. It is a subtle difference but in the case of a high-power, diode-side-pumped Nd:YAG laser it provides an input power reduction of over 8% for the PPC and nearly 5% for the APC at a target output power of 10 W. The improved efficiency is due to the better overlap with the TEM_{00} mode of the laser resonator. The coupling into the mode rather than the absorption of the pump power is the merit function for the optical pumping of a laser rod. The limitation of NERD is that it does not provide a sharp cutoff in the illumination distribution. The lack of a sharp cutoff causes a loss of pump coupling, as is evidenced in the PPC (72%) and the APC (70%) efficiencies when compared to the ERC (75%). This pump-coupling loss is more than compensated by the improved mode coupling.

Selecting a different Hermite-Gaussian mode of the laser would have altered our aim function. Rather than aiming for the center of the laser rod, we would have aimed for a point within the laser rod that overlaps better with the mode distribution. This modification can be accomplished by retaining the “source” radius term in Eq. (6) prior to integration. Additionally, the model presented herein, while extensive, does not include performance-limiting factors such as thermal birefringence, ASE, thermal expansion, and so forth. These factors have a sizable impact on the optimal pump distribution for a desired transverse mode. The inclusion of these limiting factors would improve on the modeling predictions and enable an optimal laser configuration to be designed with software prior to costly and time-consuming fabrication and experimental optimization.

NERD also has the potential to automate the reflector design process, even ones with asymmetric target distributions. An automated NERD algorithm would initially aim the light to the areas requiring the most flux. Therefore, an iterative approach for the build of the overall cross-sectional shape of the reflector would continually reassess which areas of the target need more light. Limited optimization could then be done to alter the aim function to provide better results. Finally, the NERD method gives a single, continuous reflective surface rather than a faceted structure that is prevalent in many industries, especially the automotive. The continuous surface can provide more control than is evidenced by a faceted surface.

Nonimaging concentrators such as the ERC, PPC, and APC are manufacturable by methods such as electroforming, diamond turning, injection molding, and computer-controlled milling. Of course, the PPC would prove the most demanding, and its draft release from the mold would have to be included in the design process. In the laser example studied herein, the target gain distribution is primarily affected by small-scale errors, which scatters light away from the absorber, while large-scale errors such as slope variation have a minimal effect on the laser performance. The reflectors made using these techniques typically have a very good surface quality, with roughness better than $\lambda/4$, and minimal small-scale errors. Slope errors whose correlation length approaches that of the corrugations on the concentrator surface can degrade the performance if they are of large enough magnitude. The surface tolerances in a reflector fabricated using wire-EDM of a master followed by electroforming are ± 1 deg or better for the variation of the desired slope. This variation can cause a change in the inversion density at the center of the laser by $\pm 3\%$. Our numerical modeling shows this change has minimal effect on the efficiency of the laser, and affects the

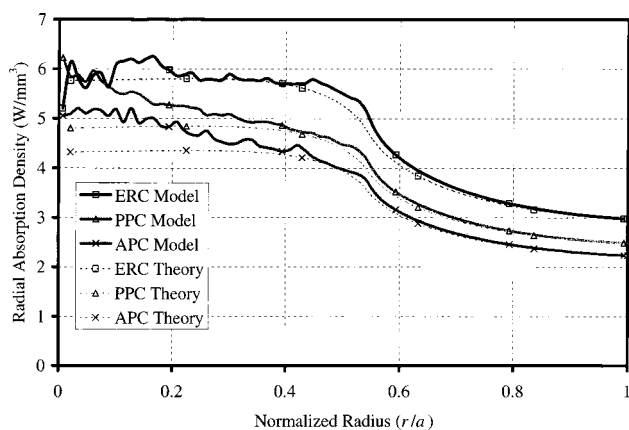


Fig. 13 Radially summed absorption distributions for the ERC, PPC, and APC designs developed herein. Additionally, an analytic model from Ref. 23 shows the distribution of absorbed power if the surface of the laser rod is Lambertian illuminated. Note the horizontal axis is normalized by the radius of the laser rod a such that values of 0.0 and 1.0 indicate the center and surface of the rod, respectively.

performance of the ERC, PPC, and APC in equal degrees. The constraints of nonimaging or pseudo-imaging systems in fabrication are greatly reduced when compared to those of imaging optics.

In summary, the PPC and APC proposed herein provides a novel solution to the problem of designing optimal pump cavities for diode-array-side pumping of solid state laser rods. The design goals of a single element consisting of a smooth, continuous reflector that gives a higher optical-optical conversion efficiency than ERC cavities are met. The design technique is quite general, and numerous other reflectors and applications can be imagined. Moreover, the method enables some control of the absorption distribution within the laser rod, so that the laser designer can to an extent mitigate undesirable effects such as thermal birefringence, ASE, higher order spatial mode losses, and so forth. In fact, one can tailor the gain profile within the active medium such that coupling into the desired output laser mode is optimized, thereby giving the most efficient laser operation for a given pump power. Future work includes tolerancing analysis of NERD pump cavities, automated design techniques, inclusion of undesirable effects, and extending modeling techniques into the temporal dynamics of the laser resonator.²⁴ The ultimate goal would be to develop an algorithm that designs, analyzes, and optimizes a laser system prior to costly and time-consuming fabrication.

Acknowledgments

This work was supported in part by CMXR, Inc, through the Small Business Innovative Research (SBIR) program when both authors were at the Institute of Optics, University of Rochester, New York. We would like to also thank the two reviewers for their helpful comments.

References

1. P. Mouroulis and J. Macdonald, *Geometrical Optics and Optical Design*, Oxford University Press, New York (1997).
2. W. T. Welford and R. Winston, *High Collection Nonimaging Optics*, Academic Press, San Diego, CA (1989).
3. D. E. Willamson, "Cone channel condenser optics," *J. Opt. Soc. Am.* **42**(10), 712–715 (1952).
4. W. Witte, "Cone channel optics," *Infrared Phys.* **5**(4), 179–185 (1965).
5. A. Rabl, "Comparison of solar energy concentrators," *Sol. Energy* **18**(2), 93–111 (1976).
6. V. K. Baranov, "Parabolotoroidal mirrors as elements of solar energy concentrators," *Appl. Sol. Energy* **2**(1), 9–12 (1966). English translation of the original article in *Geliotekhnika* **2**(1), 11–14 (1966).
7. H. Hinterberger and R. Winston, "Efficient light coupler for threshold Čerenkov counters," *Rev. Sci. Instrum.* **37**(8), 1094–1095 (1966).
8. H. C. Hottel, "Radiant energy transmission," Chap. 4 in *Heat Transmission*, 3rd ed., W. H. McAdams, Ed., pp. 55–125, McGraw-Hill, New York (1954).
9. A. Rabl, "Solar concentrators with maximal concentration for cylindrical absorbers," *Appl. Opt.* **15**(7), 1871–1873 (1976).
10. M. J. J. B. Maes and A. J. E. M. Janssen, "A note on cylindrical reflector design," *Optik (Stuttgart)* **88**(4), 177–181 (1991).
11. R. Winston and H. Ries, "Nonimaging reflectors as functionals of the desired irradiance," *J. Opt. Soc. Am. A* **10**(9), 1902–1908 (1993).
12. D. Jenkins and R. Winston, "Tailored reflectors for illumination," *Appl. Opt.* **35**(10), 1669–1672 (1996).
13. H. Ries and J. Muschaweck, "Tailored freeform optical surfaces," *J. Opt. Soc. Am. A* **19**(3), 590–595 (2002).
14. R. Burnham, "High-power transverse diode-pumped solid-state lasers," *Opt. Photonics News* **1**(8), 4–8 (1990).
15. R. J. Koshel and I. A. Walmsley, "Modeling of the gain distribution for diode pumping of a solid-state laser rod with nonimaging optics," *Appl. Opt.* **32**(9), 1517–1527 (1993).
16. D. G. Hall, "Optimum mode size criterion for low-gain lasers," *Appl. Opt.* **20**(9), 1579–1583 (1981).
17. R. J. Koshel and I. A. Walmsley, "Optimal design of optically side-pumped lasers," *IEEE J. Quantum Electron.* **33**(1), 94–102 (1997).
18. R. J. Koshel, I. A. Walmsley, R. Utano, and D. Caffey, "Diode side pumping on an Nd:YAG laser rod with a nonimaging pump cavity," in *Proc. OSA Intl. Opt. Des. Conf.* G. W. Forbes, Ed., Vol. 22, pp. 304–308 (1994).
19. T. Brand, "Compact 170-W continuous-wave diode-pumped Nd:YAG rod laser with a cusp-shaped reflector," *Opt. Lett.* **20**(17), 1776–1778 (1995).
20. R. J. Koshel, "Non-edge ray reflector design for illumination systems," *Proc. SPIE* **4092**, 71–81 (2000).
21. R. J. Koshel, "Optimal design of optically pumped lasers," PhD Thesis, University of Rochester (1996).
22. W. Koechner, *Solid-State Laser Engineering*, 4th ed., p. 94, Springer, Berlin (1996).
23. J. McKenna, "The focusing of light by a dielectric rod," *Appl. Opt.* **2**(3), 303–310 (1963).
24. R. J. Koshel, "Novel methods of intracavity beam shaping," *Proc. SPIE* **4443**, 47–57 (2001).



R. John Koshel received his BS degree in 1988 and his PhD degree in 1996 from the Institute of Optics, University of Rochester. He has since held positions in a government lab, academia, and industry. Previously he directed optical engineering services at BRO in Tucson, Arizona. He is currently with Spectrum Astro, Inc., in Tucson, where he is working on space-based optical systems. His research interests include illumination theory and design, laser design, optimization of optical systems, and ray propagation. He is also an adjunct assistant professor of optics at the Optical Sciences Center, University of Arizona, where he teaches a seminar series on illumination optics. He assists both the OSA and SPIE with leadership functions, including serving on the OPN Editorial Advisory Committee and a Chair for SPIE's "Nonimaging Optics and Efficient Illumination Design" and "Novel Optical Systems Design and Optimization Conferences."



Ian A. Walmsley received his BSc degree in physics from Imperial College, University of London, and his PhD degree from the Institute of Optics, University of Rochester. Following a brief period as a postdoctoral research associate at Cornell University he joined faculty of the Institute of Optics, and became its director in 2001. He is currently the professor of experimental physics at the University of Oxford where he is also the head of atomic and laser physics. Professor Walmsley's research interests lie in the areas of ultrafast quantum and nonlinear optics.